

# Applications of a nonlinear evolution equation I: the parton distributions in the proton

Xurong Chen<sup>1</sup>, Jianhong Ruan<sup>2</sup>, Rong Wang<sup>1,3</sup>  
Pengming Zhang<sup>1</sup> and Wei Zhu<sup>2\*</sup>

<sup>1</sup>Institute of Modern Physics, Chinese Academy of Sciences, Lanzhou 730000, P.R. China

<sup>2</sup>Department of Physics, East China Normal University, Shanghai 200062, P.R. China

<sup>3</sup> University of Chinese Academy of Sciences, Beijing, 100049, P.R. China

## Abstract

The nonlinear DGLAP evolution equations with parton recombination corrections are used to dynamically evaluate the proton's parton distribution functions starting from a low scale  $\mu^2$ , where the nucleon consists of valence quarks. We find that the resulting negative nonlinear corrections can improve the perturbative stability of the QCD evolution equation at low  $Q^2$ . Our resulting parton distributions, with four free parameters, are compatible with the existing databases. This approach provides a powerful tool to connect the quark models of the hadron and various non-perturbative effects at the scale  $\mu^2$  with the measured structure functions at the high scale  $Q^2 \gg \mu^2$ .

PACS number(s):13.60.Hb; 12.38.Bx

*keywords*: Parton distributions; QCD evolution equation; Nonlinear corrections

---

\*Corresponding author, E-mail: weizhu@mail.ecnu.edu.cn

# 1 Introduction

The parton distributions of nucleons are important components of our understanding of high energy physics. The  $Q^2$  dependence of parton densities was predicted based on a rigorous application of the renormalization group equations in QCD, guaranteeing the factorization of parton-densities in [1–3]. Currently the available parton distributions were extracted from the experimental data with the linear QCD evolution equation—the Dokshitzer-Gribov-Lipatov-Altarelli-Parisi (DGLAP) equation [1–6], which describes all results of [1–3] using an illuminating partonic picture. The solutions of the DGLAP equations depend on the initial parton distributions at low starting scale  $\mu^2$ . There are two different choices for the input distributions: (1) in global analysis, the starting point is fixed at an arbitrary scale  $Q_0^2 > 1 \text{ GeV}^2$  and the corresponding input parton distributions are parameterized by comparing with the measured data at  $Q^2 > Q_0^2$ . These input distributions are irrelevant to any physics models, one may even input negative gluon distributions; (2) in dynamical models, the parton distributions at  $Q^2 > 1 \text{ GeV}^2$  are generated by QCD radiative corrections generated from imaginary intrinsic parton distributions at an optimally determined  $Q_0^2 < 1 \text{ GeV}^2$  according to the nucleon model. For example, it is well known that the nucleons consist of three constituents at very low  $Q^2$ . A natural attempt, firstly proposed in 1977, is to assume that the nucleons consist of valence quarks at low starting point  $\mu^2$  (but still in the perturbative region  $\alpha_s(\mu^2)/2\pi < 1$  and  $\mu > \Lambda_{QCD}$ ), and the gluons and sea quarks are radioactively produced at  $Q^2 > \mu^2$  [7–9]. These input distributions allow one to construct a complete QCD picture of the proton [10–15]. However, such natural inputs fail due to overly steep behavior of the predicted parton distributions at the small Bjorken variable  $x$ . Instead of the natural inputs, Reya, Glück and Vogt (GRV) [16] added the valence like sea quarks and gluon distributions to the input parton distributions at a little larger  $Q^2$  scale. The predictions of the GRV model are compatible with the data at  $Q^2 > 4 \text{ GeV}^2$  and  $x > 10^{-4}$ .

All the above approaches determine the parton distributions via the DGLAP equation. Comparing with the natural input distributions, the valence-like distributions of the gluon and sea quarks in the GRV-model can slow down the evolution of the DGLAP equation at low  $Q^2$  and reach agreement with experimental results, since the evolution region of the valence like distributions is sizeably larger. On the other hand, we know that the contributions from the parton recombination corrections become important at  $Q^2 < 1 \text{ GeV}^2$ , which are neglected in the DGLAP equation. The correlation among initial partons can not be neglected towards small  $x$  and low  $Q^2$ . The negative corrections of the parton recombination also slow down the partons evolution. These nonlinear effects can be calculated in the perturbative QCD. The nonlinear corrections of the gluon recombination to the DGLAP equation were firstly derived by Gribov, Levin and Ryskin [17] and by Mueller and Qiu [18] in the double leading logarithmic (DLL) approximation (see Ap-

pendix A). The similar research for the nonlinear corrections to the DGLAP equation was discussed by many authors [19–21]. In particular, this evolution equation was re-derived to include parton recombination at all  $x$  by Zhu, Ruan and Shen [22–24] in the leading logarithmic (LL( $Q^2$ )) approximation. We refer to this version of the nonlinear corrections as the ZRS corrections to the DGLAP equation. Although the relation between the derivation of the nonlinear part and the renormalization group theory is unclear, in this approach [22–24] all stages of the calculation refer to parton concepts and offer a very illuminating physical interpretation of the parton recombination using the time ordered perturbative theory (TOPT).

The success of the GRV model inspires us to use natural inputs to replace the valence like inputs in the GRV model due to the nonlinear corrections of the parton recombination. Our main results are: (i) we find that the ZRS corrections suppress the fast increase of the sea quark- and gluon-densities using the natural input and has similar results as the GRV(98LO) [25] at  $x > 10^{-4}$  and  $Q^2 > 4 \text{ GeV}^2$ ; (ii) we predict that the parton distributions at  $Q^2 < 1 \text{ GeV}^2$  are positively defined, particularly, the sea quark distributions appear a plateau at small  $x$  and low  $Q^2$ , indicating Pomeron-like behavior [26]; (iii) our input quark distributions are compatible with the valence quark distributions predicted by effective chiral quark model [27]; (iv) this evidence of the parton recombination existing in the standard QCD evolution provides a possible dynamical way to explore the nuclear shadowing effects.

The organization of this paper is as follows. We present the ZRS corrections to the DGLAP equation in Sec. 2. Using the nonlinear QCD evolution equation and the natural input distributions, we calculate the evolution of the parton distributions in the proton, and the corresponding parameters are discussed in Sec. 3. Our resulting parton distributions comparing with the experimental data and some databases are presented in Sec. 4. Section 5 is the discussion and summary, where the applicability of the DGLAP equation with the ZRS corrections at the low  $Q^2$  is discussed.

## 2 The nonlinear QCD evolution equation

The DGLAP equation predicts a strong rise in the parton densities when the Bjorken variable  $x$  decrease toward small values due to the elementary process is one-parton splitting to two-partons. This behavior violates unitarity. One can expect that at very large number densities of partons, for example in the small  $x$  region, the wave functions of partons can overlap. In this case the contributions of two-partons-to-two-partons subprocesses (i.e., parton recombination) should be considered in the QCD evolution equations. Various models are proposed to modify the twist-2 DGLAP evolution kernels (i.e., the parton splitting functions). The derivation of such equations needs to sum the contributions from real and interference Feynman diagrams and corresponding virtual diagrams. Gribov, Levin and Ryskin in [17] use the AGK cutting rule [28] to count the contributions of interference diagrams. Later Mueller and Qiu [18] calculate the (real) gluon recombination functions at the double leading logarithmic approximation (DLA) in a covariant perturbation framework.

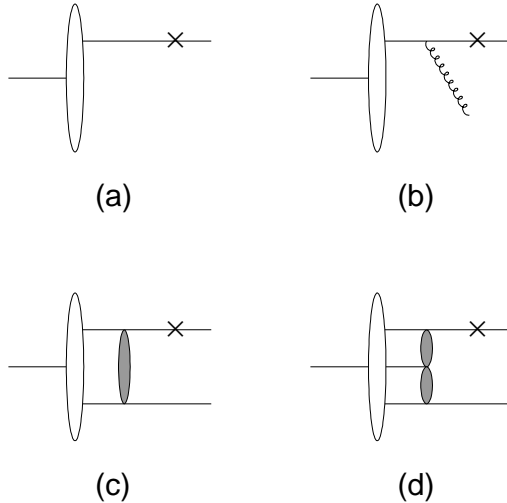


Figure 1: The elemental amplitudes, which contribute to the ZRS corrections, i.e., the corrections of the parton recombination to the standard DGLAP equation; where we have omitted the distinction between the parton flavors, "x" means the probing place and the dark circles indicate QCD interactions among all the possible correlating partons.

However, the following motivations led Zhu and his cooperators to re-derive the above QCD evolution equation with the parton recombination corrections: (1) the application of the AGK cutting rule in the GLR-MQ corrections breaks the evolution kernels (see Fig. 1 in Ref. [22]); (2) the GLR-MQ corrections to the DGLAP equation violate the momentum conservation [29]; (3) the DLL approximation is valid only at small  $x$  and the GLR-MQ corrections can not smoothly connect with the DGLAP equation [22].

To avoid these disadvantages, the relations among the relevant high twist-amplitudes are derived by using the TOPT approach at the LL( $Q^2$ ) approximation in a same framework as the derivation of the DGLAP equation in [22], where the TOPT cutting rules are proposed to connect with various cut diagrams instead of the AGK cutting rules. Thus, one can obtain the complete contributions only using the calculations of the real cut diagrams. As a consequence, a set of new evolution equations with parton recombination in a general framework was established. In next step, the the recombination functions are calculated in a whole  $x$  region based on the same TOPT-framework [23, 24].

According to the above mentioned statement, we arrange the QCD evolution equation including the ZRS corrections at the LL( $Q^2$ ) approximation for the parton distributions in a proton as follows.

We denote  $f_{v_j}(x, Q^2)$  ( $j=u,d$ ) for valence quark distributions,  $f_{q_i}(x, Q^2)$  ( $i=u,d,s$ ) for sea quark distributions,  $f_{\bar{q}_i}(x, Q^2)$  ( $i=u,d,s$ ) for anti-sea quark distributions and  $f_g(x, Q^2)$  for gluon distribution. We define  $\Sigma(x, Q^2) \equiv \sum_j f_{v_j}(x, Q^2) + \sum_i f_{q_i}(x, Q^2) + \sum_i f_{\bar{q}_i}(x, Q^2)$ . We start from the elemental amplitudes Fig. 1. According to Ref. [22], the DGLAP equation with the ZRS corrections reads

$$\begin{aligned}
& Q^2 \frac{dx f_{v_j}(x, Q^2)}{dQ^2} \\
&= \frac{\alpha_s(Q^2)}{2\pi} \int_x^1 \frac{dy}{y} P_{qq}(z) x f_{v_j}(y, Q^2) \\
&\quad - \frac{\alpha_s(Q^2)}{2\pi} x f_{v_j}(x, Q^2) \int_0^1 dz P_{qq}(z) \\
&\quad - \frac{\alpha_s^2(Q^2)}{4\pi R^2 Q^2} \int_x^{1/2} \frac{dy}{y} x P_{qg \rightarrow q}(x, y) y f_g(y, Q^2) y f_{v_j}(y, Q^2) \\
&\quad + \frac{\alpha_s^2(Q^2)}{4\pi R^2 Q^2} \int_{x/2}^x \frac{dy}{y} x P_{qg \rightarrow q}(x, y) y f_g(y, Q^2) y f_{v_j}(y, Q^2) \\
&\quad - \frac{\alpha_s^2(Q^2)}{4\pi R^2 Q^2} \int_x^{1/2} \frac{dy}{y} x P_{qq \rightarrow q}(x, y) y [\Sigma(y, Q^2) - f_{v_j}(y, Q^2)] y f_{v_j}(y, Q^2) \\
&\quad + \frac{\alpha_s^2(Q^2)}{4\pi R^2 Q^2} \int_{x/2}^x \frac{dy}{y} x P_{qq \rightarrow q}(x, y) y [\Sigma(y, Q^2) - f_{v_j}(y, Q^2)] y f_{v_j}(y, Q^2), \quad (if \ x \leq 1/2),
\end{aligned}$$

$$\begin{aligned}
& Q^2 \frac{dx f_{v_j}(x, Q^2)}{dQ^2} \\
&= \frac{\alpha_s(Q^2)}{2\pi} \int_x^1 \frac{dy}{y} P_{qq}(z) x f_{v_j}(y, Q^2) \\
&\quad - \frac{\alpha_s(Q^2)}{2\pi} x f_{v_j}(x, Q^2) \int_0^1 dz P_{qq}(z)
\end{aligned}$$

$$\begin{aligned}
& + \frac{\alpha_s^2(Q^2)}{4\pi R^2 Q^2} \int_{x/2}^{1/2} \frac{dy}{y} x P_{qg \rightarrow q}(x, y) y f_g(y, Q^2) y f_{v_j}(y, Q^2) \\
& + \frac{\alpha_s^2(Q^2)}{4\pi R^2 Q^2} \int_{x/2}^{1/2} \frac{dy}{y} x P_{qq \rightarrow q}(x, y) y [\Sigma(y, Q^2) - f_{v_j}(y, Q^2)] y f_{v_j}(y, Q^2), \text{ (if } 1/2 \leq x \leq 1),
\end{aligned} \tag{1-a}$$

for valence quarks, where  $z = x/y$ , the factor  $1/(4\pi R^2)$  is from normalizing two-parton distribution,  $R$  is the correlation length of two initial partons.

$$\begin{aligned}
& Q^2 \frac{dx f_{\bar{q}_i}(x, Q^2)}{dQ^2} \\
& = \frac{\alpha_s(Q^2)}{2\pi} \int_x^1 \frac{dy}{y} P_{qq}(z) x f_{\bar{q}_i}(y, Q^2) \\
& \quad - \frac{\alpha_s(Q^2)}{2\pi} x f_{\bar{q}_i}(x, Q^2) \int_0^1 dz P_{qq}(z) \\
& \quad + \frac{\alpha_s(Q^2)}{2\pi} \int_x^1 \frac{dy}{y} P_{qg}(z) x f_g(y, Q^2) \\
& \quad - \frac{\alpha_s^2(Q^2)}{4\pi R^2 Q^2} \int_x^{1/2} \frac{dy}{y} x P_{gg \rightarrow \bar{q}}(x, y) [y f_g(y, Q^2)]^2 \\
& \quad + \frac{\alpha_s^2(Q^2)}{4\pi R^2 Q^2} \int_{x/2}^x \frac{dy}{y} x P_{gg \rightarrow \bar{q}}(x, y) [y f_g(y, Q^2)]^2 \\
& \quad - \frac{\alpha_s^2(Q^2)}{4\pi R^2 Q^2} \int_x^{1/2} \frac{dy}{y} x P_{q\bar{q} \rightarrow \bar{q}}(x, y) y f_{q_i}(y, Q^2) y f_{\bar{q}_i}(y, Q^2) \\
& \quad + \frac{\alpha_s^2(Q^2)}{4\pi R^2 Q^2} \int_{x/2}^x \frac{dy}{y} x P_{q\bar{q} \rightarrow \bar{q}}(x, y) y f_{q_i}(y, Q^2) y f_{\bar{q}_i}(y, Q^2) \\
& \quad - \frac{\alpha_s^2(Q^2)}{4\pi R^2 Q^2} \int_x^{1/2} \frac{dy}{y} x P_{\bar{q}\bar{q} \rightarrow \bar{q}}(x, y) y [\Sigma(y, Q^2) - f_{q_i}(y, Q^2)] y f_{\bar{q}_i}(y, Q^2) \\
& \quad + \frac{\alpha_s^2(Q^2)}{4\pi R^2 Q^2} \int_{x/2}^x \frac{dy}{y} x P_{\bar{q}\bar{q} \rightarrow \bar{q}}(x, y) y [\Sigma(y, Q^2) - f_{q_i}(y, Q^2)] y f_{\bar{q}_i}(y, Q^2) \\
& \quad - \frac{\alpha_s^2(Q^2)}{4\pi R^2 Q^2} \int_x^{1/2} \frac{dy}{y} x P_{\bar{q}g \rightarrow \bar{q}}(x, y) y f_g(y, Q^2) y f_{\bar{q}_i}(y, Q^2) \\
& \quad + \frac{\alpha_s^2(Q^2)}{4\pi R^2 Q^2} \int_{x/2}^x \frac{dy}{y} x P_{\bar{q}g \rightarrow \bar{q}}(x, y) y f_g(y, Q^2) y f_{\bar{q}_i}(y, Q^2), \text{ (if } x \leq 1/2),
\end{aligned}$$

$$\begin{aligned}
& Q^2 \frac{dx f_{\bar{q}_i}(x, Q^2)}{dQ^2} \\
& = \frac{\alpha_s(Q^2)}{2\pi} \int_x^1 \frac{dy}{y} P_{qq}(z) x f_{\bar{q}_i}(y, Q^2) \\
& \quad - \frac{\alpha_s(Q^2)}{2\pi} x f_{\bar{q}_i}(x, Q^2) \int_0^1 dz P_{qq}(z)
\end{aligned}$$

$$\begin{aligned}
& + \frac{\alpha_s(Q^2)}{2\pi} \int_x^1 \frac{dy}{y} P_{qg}(z) x f_g(y, Q^2) \\
& + \frac{\alpha_s^2(Q^2)}{4\pi R^2 Q^2} \int_{x/2}^{1/2} \frac{dy}{y} x P_{gg \rightarrow \bar{q}}(x, y) [y f_g(y, Q^2)]^2 \\
& + \frac{\alpha_s^2(Q^2)}{4\pi R^2 Q^2} \int_{x/2}^{1/2} \frac{dy}{y} x P_{q\bar{q} \rightarrow \bar{q}}(x, y) y f_{q_i}(y, Q^2) y f_{\bar{q}_i}(y, Q^2) \\
& + \frac{\alpha_s^2(Q^2)}{4\pi R^2 Q^2} \int_{x/2}^{1/2} \frac{dy}{y} x P_{q\bar{q} \rightarrow \bar{q}}(x, y) y [\Sigma(y, Q^2) - f_{q_i}(y, Q^2)] y f_{\bar{q}_i}(y, Q^2) \\
& + \frac{\alpha_s^2(Q^2)}{4\pi R^2 Q^2} \int_{x/2}^{1/2} \frac{dy}{y} x P_{qg \rightarrow \bar{q}}(x, y) y f_g(y, Q^2) y f_{\bar{q}_i}(y, Q^2), \quad (if \ 1/2 \leq x \leq 1), \quad (1-b)
\end{aligned}$$

for sea quark distributions and

$$\begin{aligned}
& Q^2 \frac{dx f_g(x, Q^2)}{dQ^2} \\
& = \frac{\alpha_s(Q^2)}{2\pi} \int_x^1 \frac{dy}{y} P_{gq}(z) x \Sigma(y, Q^2) \\
& + \frac{\alpha_s(Q^2)}{2\pi} \int_x^1 \frac{dy}{y} P_{gg}(z) x f_g(y, Q^2) \\
& - f \frac{\alpha_s(Q^2)}{2\pi} x f_g(x, Q^2) \int_0^1 dz P_{qg}(z) \\
& - \frac{1}{2} \frac{\alpha_s(Q^2)}{2\pi} x f_g(x, Q^2) \int_0^1 dz P_{gg}(z) \\
& - \frac{\alpha_s^2(Q^2)}{4\pi R^2 Q^2} \int_x^{1/2} \frac{dy}{y} x P_{gg \rightarrow g}(x, y) [y f_g(y, Q^2)]^2 \\
& + \frac{\alpha_s^2(Q^2)}{4\pi R^2 Q^2} \int_{x/2}^x \frac{dy}{y} x P_{gg \rightarrow g}(x, y) [y f_g(y, Q^2)]^2 \\
& - \frac{\alpha_s^2(Q^2)}{4\pi R^2 Q^2} \int_x^{1/2} \frac{dy}{y} x P_{q\bar{q} \rightarrow g}(x, y) \sum_{i=1}^f [y f_{\bar{q}_i}(y, Q^2)]^2 \\
& + \frac{\alpha_s^2(Q^2)}{4\pi R^2 Q^2} \int_{x/2}^x \frac{dy}{y} x P_{q\bar{q} \rightarrow g}(x, y) \sum_{i=1}^f [y f_{\bar{q}_i}(y, Q^2)]^2 \\
& - \frac{\alpha_s^2(Q^2)}{4\pi R^2 Q^2} \int_x^{1/2} \frac{dy}{y} x P_{qg \rightarrow g}(x, y) y \Sigma(y, Q^2) y f_g(y, Q^2) \\
& + \frac{\alpha_s^2(Q^2)}{4\pi R^2 Q^2} \int_{x/2}^x \frac{dy}{y} x P_{qg \rightarrow g}(x, y) y \Sigma(y, Q^2) y f_g(y, Q^2), \quad (if \ x \leq 1/2),
\end{aligned}$$

$$Q^2 \frac{dx f_g(x, Q^2)}{dQ^2}$$

$$\begin{aligned}
&= \frac{\alpha_s(Q^2)}{2\pi} \int_x^1 \frac{dy}{y} P_{gq}(z) x \Sigma(y, Q^2) \\
&+ \frac{\alpha_s(Q^2)}{2\pi} \int_x^1 \frac{dy}{y} P_{gg}(z) x f_g(y, Q^2) \\
&- f \frac{\alpha_s(Q^2)}{2\pi} x f_g(x, Q^2) \int_0^1 dz P_{qg}(z) \\
&- \frac{1}{2} \frac{\alpha_s(Q^2)}{2\pi} x f_g(x, Q^2) \int_0^1 dz P_{gg}(z) \\
&+ \frac{\alpha_s^2(Q^2)}{4\pi R^2 Q^2} \int_{x/2}^{1/2} \frac{dy}{y} x P_{gg \rightarrow g}(x, y) [y f_g(y, Q^2)]^2 \\
&+ \frac{\alpha_s^2(Q^2)}{4\pi R^2 Q^2} \int_{x/2}^{1/2} \frac{dy}{y} x P_{q\bar{q} \rightarrow g}(x, y) \sum_{i=1}^f [y f_{\bar{q}_i}(y, Q^2)]^2 \\
&+ \frac{\alpha_s^2(Q^2)}{4\pi R^2 Q^2} \int_{x/2}^{1/2} \frac{dy}{y} x P_{qg \rightarrow g}(x, y) y \Sigma(y, Q^2) y f_g(y, Q^2), \quad (if \ 1/2 \leq x \leq 1), \quad (1-c)
\end{aligned}$$

for gluon distribution. The corresponding cut diagrams are presented in Fig. 2. Note that the TOPT cutting rules [22] are used in Eq. (1). Thus, we need only compute the two-partons to two-partons kernels and use the same kernels to write the contributions of the interference processes. On the other hand, the contributions of the virtual processes are canceled each other [22].

The un-regularized DGLAP splitting kernels in the linear terms are [22, 30, 31]

$$P_{gg}(z) = 2C_A \left[ z(1-z) + \frac{1-z}{z} + \frac{z}{1-z} \right],$$

$$P_{gq}(z) = C_F \frac{1 + (1-z)^2}{z},$$

$$P_{qq}(z) = C_F \frac{1+z^2}{1-z},$$

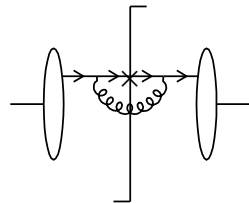
$$P_{qg}(z) = T_R [z^2 + (1-z)^2], \quad (2)$$

where  $C_A = N_c = 3$ ,  $C_F = \frac{N_c^2 - 1}{2N_c} = \frac{4}{3}$ ,  $T_R = \frac{1}{2}$  and  $z = x/y$ .

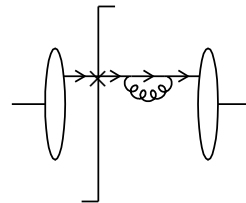
The recombination functions (Fig. 3) in the nonlinear terms are

$$P_{gg \rightarrow g}(x, y) = \frac{9}{64} \frac{(2y-x)(72y^4 - 48xy^3 + 140x^2y^2 - 116x^3y + 29x^4)}{xy^5},$$

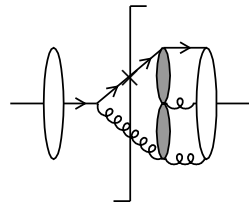
$$P_{gg \rightarrow q}(x, y) = P_{gg \rightarrow \bar{q}}(x, y) = \frac{1}{96} \frac{(2y-x)^2(18y^2 - 21xy + 14x^2)}{y^5},$$



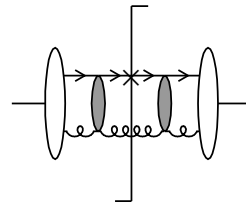
(a)  $v \rightarrow vg$



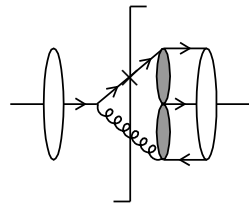
(b)  $v \rightarrow vg$



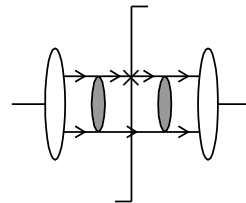
(c)  $vg \rightarrow vg$



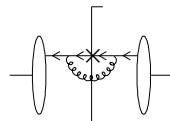
(d)  $vg \rightarrow vg$



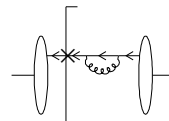
(e)  $v\Sigma \rightarrow v\Sigma$



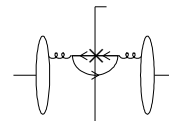
(f)  $v\Sigma \rightarrow v\Sigma$



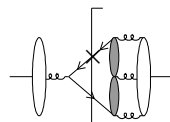
(a)  $\bar{q} \rightarrow \bar{q}g$



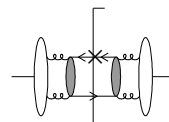
(b)  $\bar{q} \rightarrow \bar{q}g$



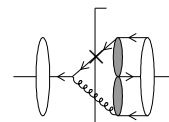
(c)  $g \rightarrow \bar{q}q$



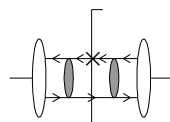
(d)  $gg \rightarrow \bar{q}q$



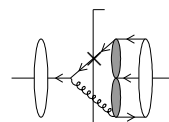
(e)  $gg \rightarrow \bar{q}q$



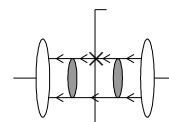
(f)  $\bar{q}q \rightarrow \bar{q}q$



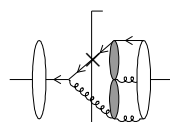
(g)  $\bar{q}q \rightarrow \bar{q}q$



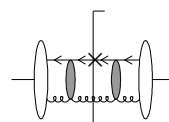
(h)  $\bar{q}q \rightarrow \bar{q}q$



(i)  $\bar{q}q \rightarrow \bar{q}q$



(j)  $\bar{q}g \rightarrow \bar{q}g$



(k)  $\bar{q}g \rightarrow \bar{q}g$

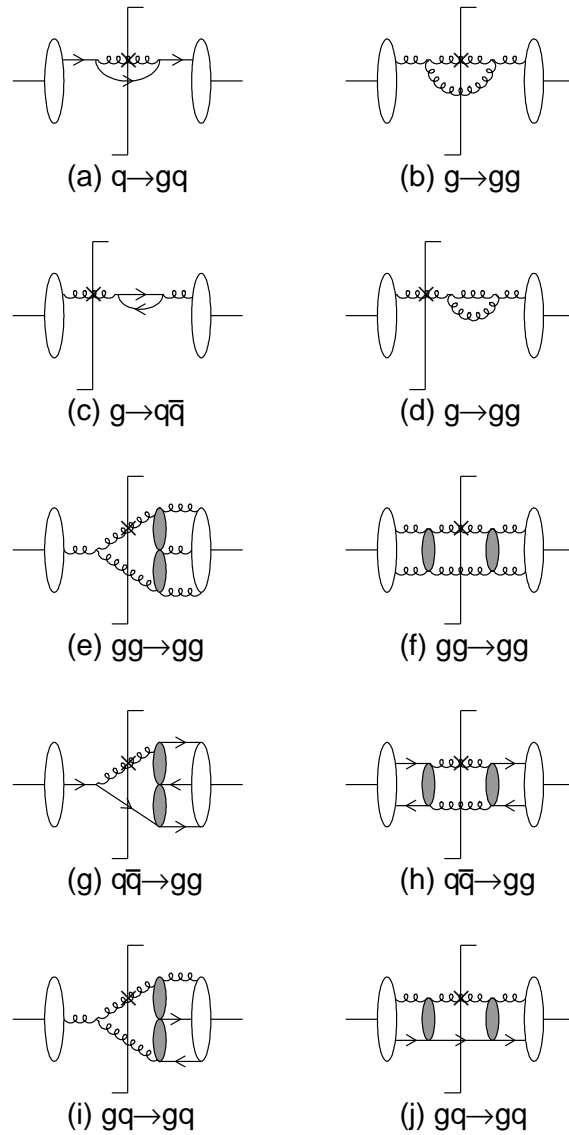


Figure 2: The cut diagrams for the DGLAP equation with the ZRS corrections using the elemental amplitudes in Fig. 1.

$$\begin{aligned}
P_{qq \rightarrow q}(x, y) &= P_{\bar{q}\bar{q} \rightarrow \bar{q}}(x, y) = \frac{2}{9} \frac{(2y-x)^2}{y^3}, \\
P_{q\bar{q} \rightarrow q}(x, y) &= P_{q\bar{q} \rightarrow \bar{q}}(x, y) = \frac{1}{108} \frac{(2y-x)^2(6y^2+xy+3x^2)}{y^5}, \\
P_{qg \rightarrow q}(x, y) &= P_{\bar{q}g \rightarrow \bar{q}}(x, y) = \frac{1}{288} \frac{(2y-x)(140y^2-52yx+65x^2)}{y^4}, \\
P_{qg \rightarrow g}(x, y) &= P_{\bar{q}g \rightarrow g}(x, y) = \frac{1}{288} \frac{(2y-x)(304y^2-202yx+79x^2)}{xy^4}, \\
P_{q\bar{q} \rightarrow g}(x, y) &= \frac{4}{27} \frac{(2y-x)(18y^2-9yx+4x^2)}{xy^3},
\end{aligned} \tag{3}$$

they are taken from Ref. [23].

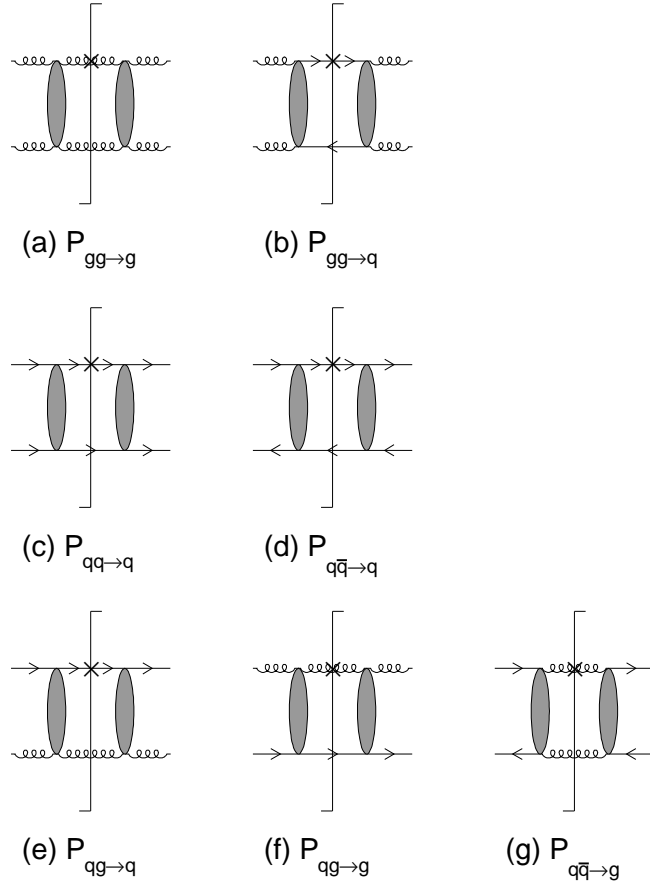


Figure 3: The recombination functions in Eq. (3), which are calculated at LL( $Q^2$ )A in Ref. [12].

The properties of the equation (1-3) are summarized as follows.

(1) The QCD evolution kernels (for example, splitting function in the DGLAP equation and recombination functions in the corrected equation) are separated from the coefficient functions using the equivalent particle approximation [32–35]. However, the infrared (IR) divergence due to the gauge singularities in some twist-4 amplitudes prevents us from using the equivalent particle approximation, since these gauge terms are coupled with the backward components of two parton legs which connect with the probe. In the derivation of the GLR-MQ corrections, the gauge singularities become finite using a contour integral. In this method, the backward components of two legs still exist, i.e., the propagators of the legs are off-mass-shell. This implies that the equivalent particle approximation is invalid. On the other hand, the gauge singularities in the twist-4 coefficient functions are safely removed from the ZRS corrections using the TOPT method. Thus, the recombination kernels can be simply separated from the coefficient functions at the equivalent particle approximation. A detailed discussion see Ref. [24].

(2) The equation is a result summing all possible cut diagrams up to twist-4 in a quantum field theory framework (i.e., the TOPT) instead of using the AGK cutting rules. The two-parton-to-two-parton amplitude leads to the positive (antishadowing) effect, while the contributions of interference amplitudes between the one-parton-to-two-partons and the three-partons-to-two-partons processes yield a negative (shadowing) effect. The co-existence of shadowing and antishadowing in the QCD evolution of the parton densities is a general requisition of the local momentum conservation [29]. We emphasize that the shadowing and antishadowing terms are defined on different kinematic domains  $[x, 1/2]$  and  $[x/2, x]$ , respectively. Thus, the momentum is conservative as shown in following Eq. (4). On the other hand, the AGK cutting rule is used in the derivation of the GLR-MQ corrections, where the contributions of the positive and negative terms only differ in the numerical weights. Thus, the antishadowing effect in the GLR-MQ corrections is completely canceled by the effect and the resulting evolution equation violates the momentum conservation.

(3) Since Eqs. (1)-(3) are derived at the  $LL(Q^2)$  approximation and they contain the terms beyond the DLL approximation, the DGLAP equation with the ZRS corrections is valid in the full- $x$  range if we neglect the Balitsky- Fadin-Kuraev-Lipatov (BFKL) corrections [36–41] at the very small- $x$  region. Thus, the ZRS corrections can smoothly connect with the DGLAP equation.

(4) The sea quark evolutions in the ZRS corrections (1-b) and GLR-MQ corrections (A-2) (see Appendix A) take different forms. The reason is that the transition of gluon-quarks is suppressed in the DLLA manner. The DLLA diagram contains only the gluon ladders and any transitions of gluon-quark break the gluon ladder structure. Therefore, a special box diagram is used to include the corrections of gluon recombination to the quark distributions in the GLR-MQ corrections. However, this extra diagram is unnecessary in

the derivation of the ZRS corrections, since we can produce the evolution equations for gluon and sea quarks in the same framework at the LL( $Q^2$ ) approximation.

(5) The combining distribution of two partons, for say two gluons, is assumed to be  $f_g^{(2)}(y, Q^2) \sim f_g^2(y, Q^2)$  either in the ZRS corrections or in the GLR-MQ corrections. This is a simplest model. One of us (W.Z.) has discussed the recombination of gluons with different values of  $x$  in the nonlinear evolution equation and finds that this modification unreasonably enhances the shadowing effect in the GLR-MQ corrections, while it does not change the predictions of the ZRS corrections, since the momentum conservation plays an important role in this result [42].

Comparing with the GLR-MQ corrections, the ZRS corrections reasonably describe the corrections of the parton recombination to the DGLAP equation at the twist-4 level. The DGLAP equation with the ZRS corrections has been applied to study some small  $x$  phenomena in its approximation form [43–46]. In this work we will use its complete version Eq. (1-3) to quantitatively study the parton distributions in the proton.

### 3 Natural initial distributions and free parameters fitting

The solutions of the QCD evolution equations for the parton distributions depend on the initial parton distributions at a low scale  $Q^2 = \mu^2$ . An ideal and simple assumption is that the nucleon consists entirely of three valence quarks at  $\mu^2$  and the gluon and sea distributions at  $Q^2 > \mu^2$  are generated radioactively. This naive model was firstly proposed in Refs. [7–9] and it successfully predicts that at low  $Q^2 \sim 1 \text{ GeV}^2$  about 50% of the nucleon momentum is already carried by gluons, which agrees with the experimental results. Unfortunately, the distributions of the sea quarks and gluon predicted by this natural input and the DGLAP equation are too steep. Instead of the simple input distributions, Glück, Reya and Vogt (GRV) [16] assumed that the nucleon has valence quarks and special valence-like sea quarks and valence-like gluon at a starting point at  $Q^2 \simeq 0.2 \sim 0.3 \text{ GeV}^2$ . The GRV input in the DGLAP equation nicely predicts the parton distributions in a broad kinematical range.

Now we go back to the natural input distributions with the ZRS corrections using Eqs. (1-3) for the second moments of the distributions and the measured momentum of the valence quark distributions at a higher  $Q^2$ , we obtain the starting point  $\mu^2 = 0.064 \text{ GeV}^2$  (with  $\Lambda_{QCD} = 0.204 \text{ GeV}$  for  $f=3$  flavors). Note that the value of  $1/\mu \sim 0.8 fm$  is compatible with a typical radius of the proton. This value of  $\mu$  is similar to the previous estimation in Refs. [7–9], where the DGLAP equation is used. The reason is that the contributions of the nonlinear (shadowing and antishadowing) terms to the  $Q^2$ -evolution of the momentum fractions in the ZRS corrections vanish due to the momentum conservation [22]

$$\begin{aligned}
 & -\frac{\alpha_s^2(Q^2)}{4\pi R^2 Q^2} \int_0^{1/2} dx \int_x^{1/2} \frac{dy}{y} x P_{qg \rightarrow q}(z) [y f_g(y, Q^2) y f_v(y, Q^2)] \\
 & + \frac{\alpha_s^2(Q^2)}{4\pi R^2 Q^2} \int_0^{1/2} dx \int_{x/2}^x \frac{dy}{y} x P_{qg \rightarrow q}(z) [y f_g(y, Q^2) y f_v(y, Q^2)] \\
 & + \frac{\alpha_s^2(Q^2)}{4\pi R^2 Q^2} \int_{1/2}^1 dx \int_{x/2}^{1/2} \frac{dy}{y} x P_{qg \rightarrow q}(z) [y f_g(y, Q^2) y f_v(y, Q^2)] = 0.
 \end{aligned} \tag{4}$$

According to the natural input distribution,

$$f_g(x, \mu^2) = 0, \quad f_{q_i}(x, \mu^2) = f_{\bar{q}_i}(x, \mu^2) = 0. \tag{5}$$

We choose a minimum free parameter scheme for the typical valence quark distributions

$$x f_{v_u}(x, \mu^2) = A_u x^{B_u} (1-x)^{C_u},$$

$$xf_{v_d}(x, \mu^2) = A_d x^{B_d} (1-x)^{C_d}, \quad (6)$$

which satisfy the momentum sum rule

$$\int_0^1 dx x [f_{v_u}(x, \mu^2) + f_{v_d}(x, \mu^2)] = 1. \quad (7)$$

and the normalization conditions

$$\int_0^1 dx f_{v_u}(x, \mu^2) = 2, \quad \int_0^1 dx f_{v_d}(x, \mu^2) = 1. \quad (8)$$

Fitting to experimental data, we obtain following values for the proton  $A_u = 24.30$ ,  $B_u = 1.98$ ,  $C_u = 2.06$ ,  $A_d = 9.10$ ,  $B_d = 1.31$ , and  $C_d = 3.80$ .

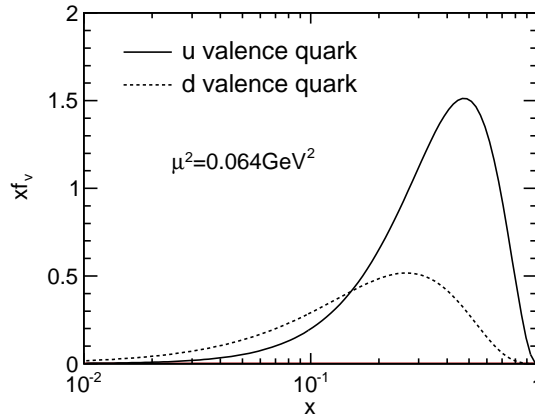


Figure 4: The natural input distributions in the proton at the initial scale  $\mu^2 = 0.064$  GeV<sup>2</sup>.

The corresponding input distributions are shown in Fig. 4. The free parameter  $R$  in Eq.(1) depends on the geometric distributions of partons inside the proton.  $R \simeq 5$  GeV<sup>-1</sup> (or  $R < 5$  GeV<sup>-1</sup>) when the partons distribute uniformly (or non-uniformly) in the proton. We take  $R = 4.24$  GeV<sup>-1</sup> for best fitting to the data.

## 4 Parton distributions in the proton

Since the four free parameters are fixed, now it is straightforward to calculate the evolution of the parton distributions in the proton using Eqs. (1-3). The  $x$  and  $Q^2$  dependence of our predicted structure functions and comparisons with the data [47–59] are shown in Figs. 5 and 6. Our results are generally lower than the experimental data at  $x < 10^{-4}$ . It implies that the BFKL correction is not negligible in such small  $x$  range.

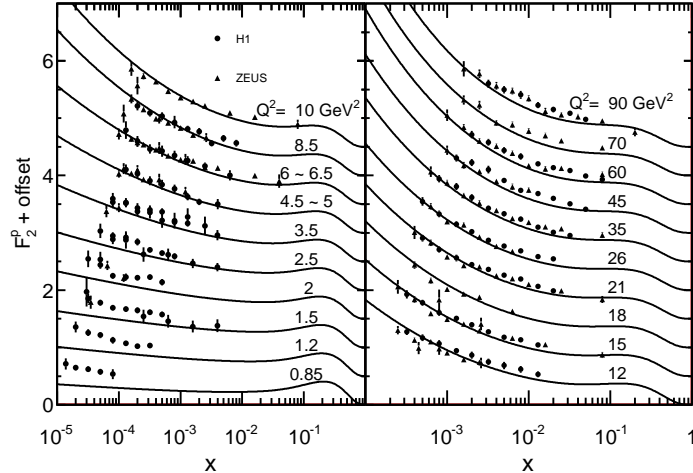


Figure 5: Comparisons of our predicted  $x$ -dependence of  $F_2^p(x, Q^2)$  (solid curves) with HERA data [47–56] at small  $x$ .

The comparisons of two dynamically generated parton distributions of the proton (i.e., using Eqs. (1-3) with the natural input and using the DGLAP equation with the GRV(98LO) input) are shown in Figs. 7-10. In Figs. 9 and 10 we plot the parton distributions in the linear DGLAP equation with the natural input. One can find that the valence like input distributions in the GRV model are equivalent to the effective description of the nonlinear parton recombination.

We try to explore the parton distributions down to  $Q^2 < 1 \text{ GeV}^2$  at small  $x$  using Eqs. (1-3). Our predicted proton structure functions are shown in Fig. 11, where we plot the contributions of the Regge part in the Donnachie-Landshoff (DL) model [60]. The prediction of gluon and sea quark distributions at low  $Q^2$  based on Eqs. (1-3) is presented in Fig. 12. Although the predicted structure functions are lower than the ZEUS data [52–56], the plateau-like shapes allow us to establish a smooth connection between the partonic and non-partonic pictures of the nucleon’s structure functions in low  $Q^2$  and small  $x$  range [61]. It will be studied in our following work.

The difference between our model and GRV model becomes obvious near the GRV starting point  $Q^2 \simeq 0.26 \text{ GeV}^2$  (Fig. 13). The comparisons of our model with the GRV

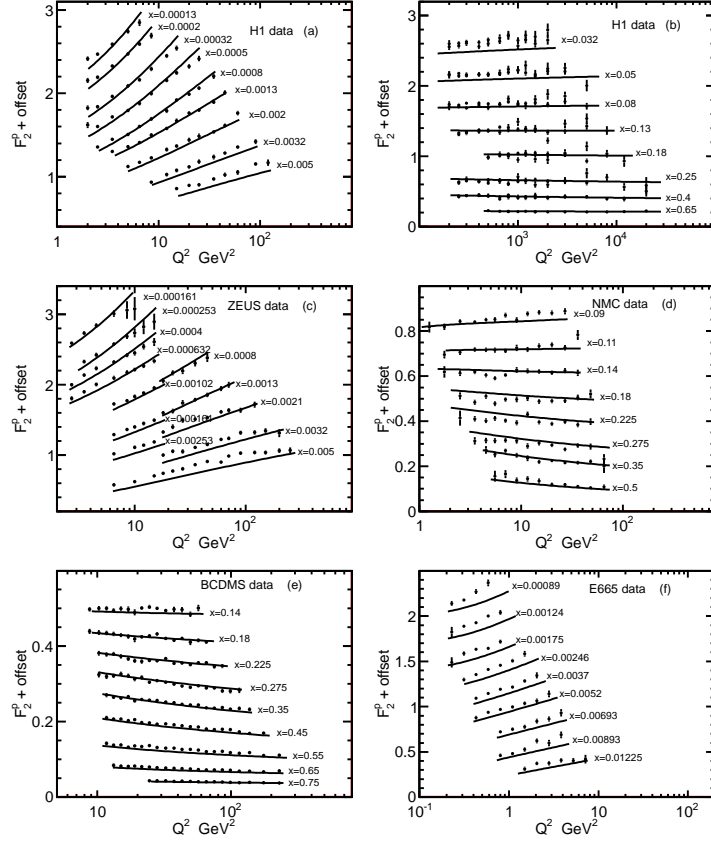


Figure 6: Comparisons of our predicted  $Q^2$ -dependence of  $F_2^p(x, Q^2)$  (solid curves) with various experimental data [47–59].

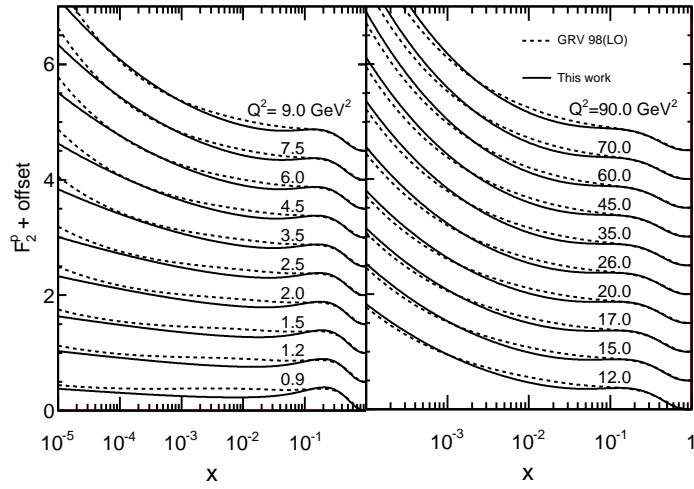


Figure 7: Comparisons of the  $x$ -dependence of our predicted  $F_2^p$  (solid curves) with the GRV(98LO) results (dashed curves) [25].

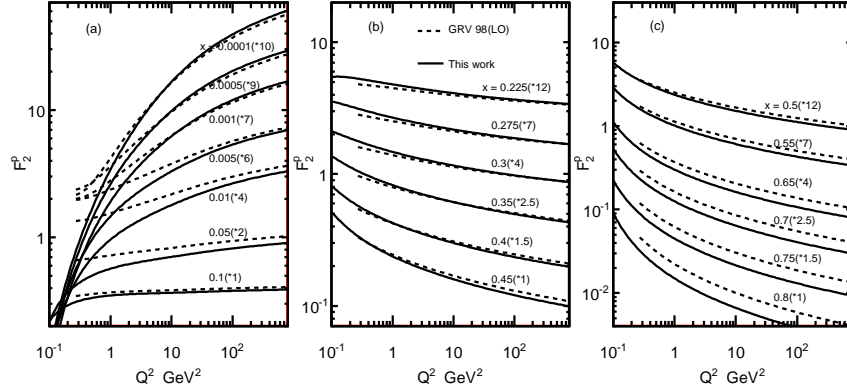


Figure 8: Comparisons of the  $Q^2$ -dependence of our predicted  $F_2^P$  (solid curves) with the GRV(98LO) results (dashed curves) [25]. For a better display, the structure function values are scaled at each  $x$  by the factors shown in brackets.

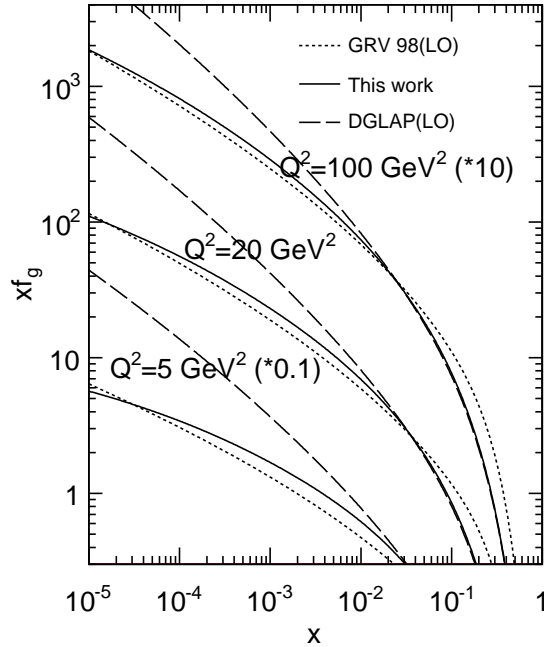


Figure 9: Comparisons among our predicted gluon distribution (solid curves), the GRV(98LO) (dashed curves) [25] and the results using the DGLAP evolution with the natural input (broken curves).

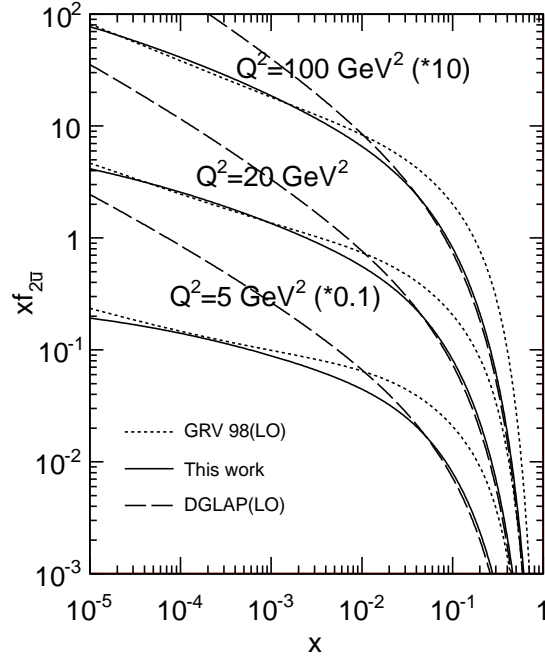


Figure 10: Similar to Fig. 9, but for the sea quark distributions.

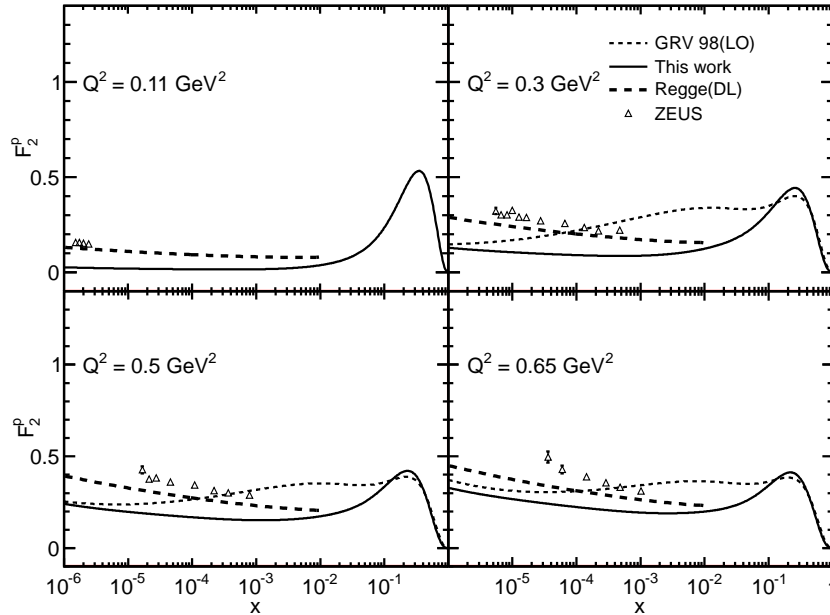


Figure 11: Our predicted proton structure function (solid curves) in low  $Q^2$  range. The contributions of Regge part in the Donnachie-Landshoff model (broken curves) [60], GRV(98LO) [25] results (dashed curves) and the ZEUS data [52–56] are presented.

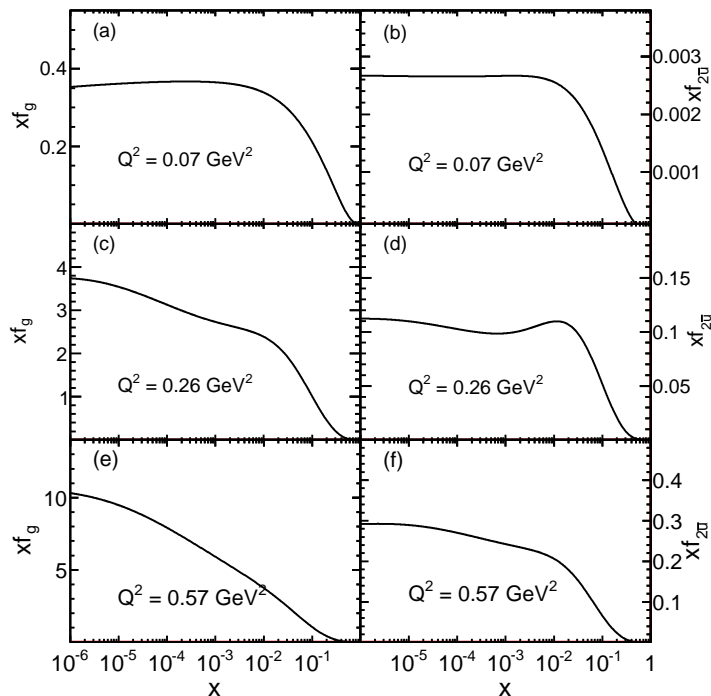


Figure 12: Our predicted gluon (Left) and sea quarks (Right) distributions in the low  $Q^2$  range.

and CJ12 [62] databases at  $Q^2 = 1.4 \text{ GeV}^2$  are presented in Fig. 14.

The predicted gluon distributions of the different databases exhibit large difference. The reason is that the lepton probes can not directly measure the gluon distribution. The parameters of input gluon distribution are determined by higher order QCD processes, such as the scaling violation and longitudinal structure function  $F_L$ . Because only limited amount of data are available, the constraints on the input gluon distribution are much looser than for quarks. Different from those global databases, both gluon and sea quarks are dynamically generated from the input valence quarks based on Eqs. (1-3) in this work. Once the valence quark input is fixed by the observed quark distributions, the gluon distribution is also determined in the leading order. The comparisons of the  $x$ -dependence of the gluon distributions at given  $Q^2$  are plotted in Figs. 15-17.

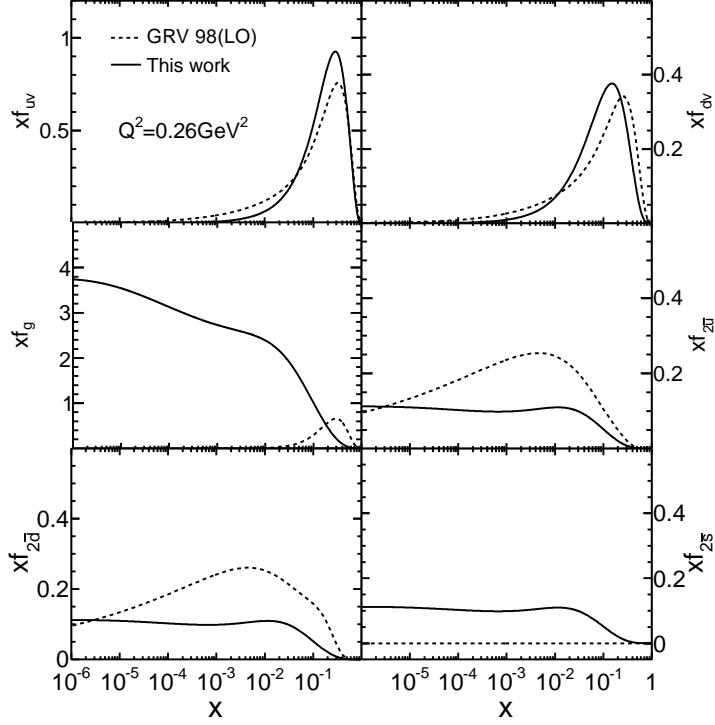


Figure 13: Comparisons of our predicted parton distributions (solid curves) with the GRV input (dashed curves) at the GRV-starting point  $Q^2 = 0.26 \text{ GeV}^2$ .

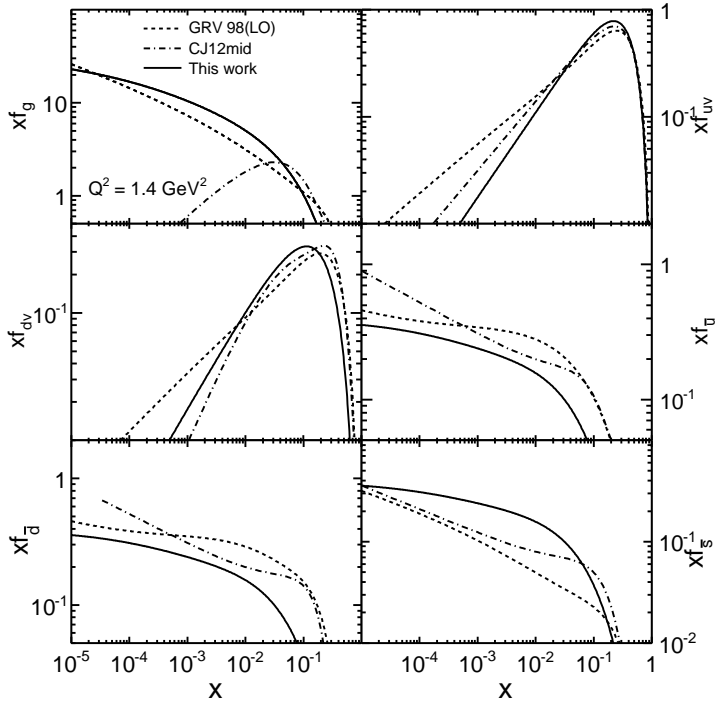


Figure 14: Comparisons of our predicted parton distributions (solid curves) with GRV98 [25] and CJ12 [62] distributions at  $Q^2 = 1.4 \text{ GeV}^2$ .

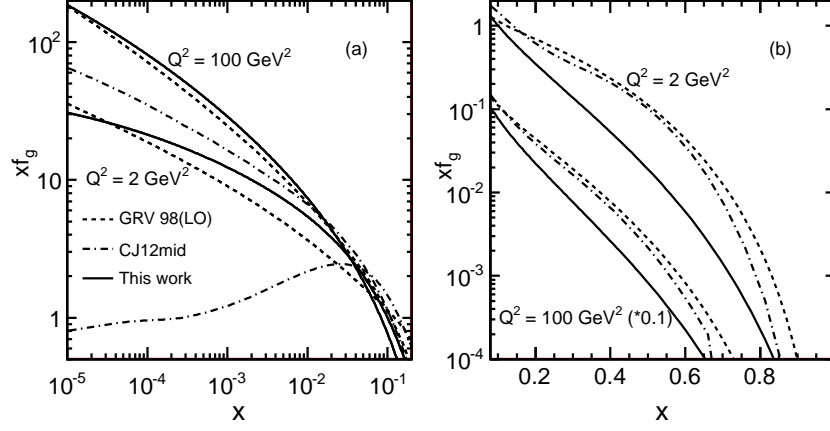


Figure 15: Comparisons of our predicted  $x$ -dependence of gluon distribution (solid curves) with GRV98 [25] and CJ12 [62] distributions at different  $Q^2$ .

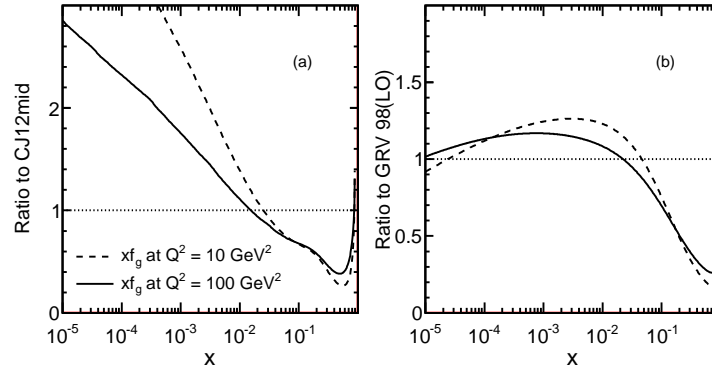


Figure 16: Ratios of our predicted gluon distribution to (a) CJ12 [62] and (b) GRV98 [25] distributions at  $Q^2 = 10$  and  $100 \text{ GeV}^2$ .

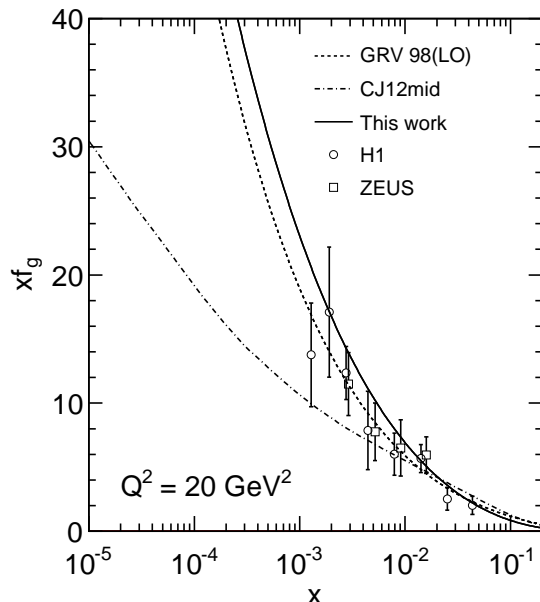


Figure 17: Comparisons of our predicted gluon distribution at  $Q^2 = 20 \text{ GeV}^2$  with the HERA data. The results of GRV98 [25] and CJ12 [62] gluon distributions also are presented.

## 5 Discussions and Summary

An unavoidable question is whether Eq. (1) can be used at  $Q^2 \geq 0.064 \text{ GeV}^2$ . Now let us discuss this question.

One may think that a large value of  $\alpha_s$  at low  $Q^2$  will lead to a divergent perturbative expansion. Refs. [7–9] have emphasized that the DGLAP evolution is still in the perturbative region even at low static point  $\mu^2 \sim 0.064 \text{ GeV}^2$  since the expansion factor is  $\alpha_s(\mu^2)/2\pi < 1$  in the DGLAP equation and the evolution kernels are non-singular at low  $Q^2$ . The GRV model was extended to the next leading order and even to the next-next leading order approximation at  $Q^2 < 1 \text{ GeV}^2$  [63]. These results indicate that the higher order corrections to the DGLAP evolution are small.

We show that these conclusions are still valid for the DGLAP equation with the ZRS corrections. The perturbative approximation may be invalid if the net (shadowing and antishadowing) effect is positive. As we have pointed out that the size of the ZRS correction is not only dependent on the magnitude of  $\alpha_s(Q^2)$ , but also is related to the shape of the parton densities in the range of  $x$  to  $x/2$  [65]. The net nonlinear correction will be positive if the parton distribution  $\sim x^{-\lambda}$  ( $\lambda > \lambda_{BFKL} \sim 0.5$ ). However, the radioactively generated partons by the DGLAP evolution at small  $x$  behave as  $\sim x^{-\lambda}$  ( $\lambda < \lambda_{BFKL}$ ) even through it is steep. In this case the shadowing effect in the evolution

process will be weakened by the antishadowing effect, and the net effect of the parton fusions always keeps the negative correction. The parton distributions will asymptotically approach a finite value by the action of the net shadowing in the leading order level. On the other hand, the contributions of the higher order recombination (i.e., the multi-parton recombination) is negligible since the parton densities are low at  $Q^2 < 1 \text{ GeV}^2$ . We also notice the possibility that the nonperturbative dynamics of QCD generates an effective gluon mass at very low  $Q^2$  region [35], or gluons become Abelian gluons when  $Q^2 \rightarrow \Lambda_{QCD}^2$  [69, 70]. A simple phenomenological approach can be used to estimate the above corrections to the evolution of the parton distributions: the QCD running coupling constant is frozen at an infrared value, i.e.,  $\alpha_s(Q^2) \leq \kappa$ ,  $\kappa$  is an undetermined parameter. Using this restriction we obtain the similar results after adjusting the input distributions. Our numerical calculations also show that the resummations  $\sum_n [\alpha_s/(2\pi) \ln(Q^2/\Lambda_{QCD})]^n$  and  $\sum_n [\alpha_s^2/(4\pi R^2 Q^2)]^n$  converge quickly, i.e., the perturbative evolution of Eq. (1) is stable at low  $Q^2$ .

Our analysis has shown that the parton recombination plays an important role at small  $x$  and low  $Q^2$ . Although any power law correction including parton recombination will disappear at high  $Q^2$ , the contributions of the nonlinear terms in Eq.(1) at low  $Q^2$  will be "remembered" in the parton distribution evolution process and observed at high  $Q^2$ . For example, with the same natural input distribution there is a big difference between the parton distributions from the DGLAP equation and the ones from Eqs. (1-3), as shown in Figs. 9 and 10.

The input valence quark distributions parameterize the interactions of constituents of the proton at scale  $Q^2 \rightarrow \Lambda_{QCD}$  in the strong coupling regime. One can use chiral effective field theories to model the input valence quark distributions as Ref. [27]. It is interesting to notice that these distributions are compatible with our parameterized input shown in Fig. 18. Therefore, we think that the DGLAP equation with the ZRS corrections is a powerful tool to connect the effective QCD quark model of hadron at scale  $\mu^2$  with the observed structure function at high scale  $Q^2 \gg \mu^2$ .

The parton distributions of the proton in this work can be generalized to nuclear target, where the nuclear shadowing effect is a natural result of the parton recombination among different bound nucleons, while the nuclear environment deforms the input valence quarks. We will discuss them in our next work.

In this work, all sea quarks are generated perturbatively by gluon splitting. Therefore, the sea quark distributions have isospin symmetry. However, experiments questioned these naive expectations [71, 72]. These effects require nonperturbative explanations. In this respect, the DGLAP equation with ZRS corrections provides an effective way to test various models which may modify the input distributions. Furthermore, in our following works, the results of this work will be used to dynamically predict the nuclear gluon

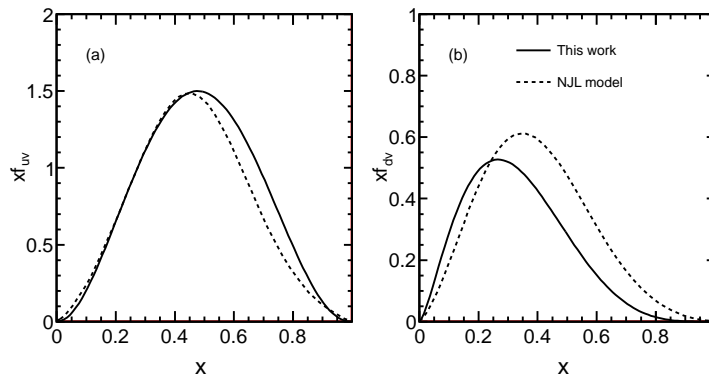


Figure 18: Comparisons of our input quark distributions (solid curves) with the valence quark distributions in the Nambu-Jona-Lasinio model (dashed curves) [27].

distributions and to reduce the free parameters related to EMC effects.

In summary, the parton distributions in the proton are evaluated dynamically starting from three valence quarks input at the low scale  $\mu^2$  by the DGLAP equation with the ZRS corrections. Our results show that negative nonlinear corrections improve the perturbative stability of the QCD evolution equation at low  $Q^2$ . Our predicted parton distributions of the proton with four free parameters are compatible with the existing databases. We show that the sea quark distributions exhibit a positive and plateau-like behavior at small  $x$  and low  $Q^2$ . This approach provides a powerful tool to connect the quark models of the hadron and various non-perturbative effects at the scale  $\mu^2$  with the measured structure functions at the high scale  $Q^2 \gg \mu^2$ .

**Acknowledgments:** This work is partly supported by the National Natural Science Foundations of China under the Grants Number 10875044, 11275120 and Century Program of Chinese Academy of Sciences Y101020BR0.

## Appendix A. The GLR-MQ corrections.

For comparing with the ZSR corrections, we present the GLR-MQ corrections to the DGLAP equation at the DLL approximation [9]

$$\begin{aligned}
& Q^2 \frac{dx f_g(x, Q^2)}{dQ^2} \\
= & Q^2 \frac{dx f_g(x, Q^2)}{dQ^2} \Big|_{DGLAP} - \frac{9\alpha_s^2(Q^2)}{2R^2 Q^2} \int_x^{10^{-2}} \frac{dy}{y} [y f_g(y, Q^2)]^2, \tag{A-1}
\end{aligned}$$

$$\begin{aligned}
& Q^2 \frac{dx f_{\bar{q}_i}(x, Q^2)}{dQ^2} \\
= & Q^2 \frac{dx f_{\bar{q}_i}(x, Q^2)}{dQ^2} \Big|_{DGLAP} - \frac{3\alpha_s^2(Q^2)}{20R^2 Q^2} [xg(x, Q^2)]^2 \\
+ & \frac{6\alpha_s}{\pi Q^2} \int_x^{10^{-2}} \frac{dy}{y} \frac{-2y^3 x^2 + 15y^2 x^3 - 30yx^4 + 18x^5}{y^5} y G_{HT}(y, Q^2) \tag{A-2},
\end{aligned}$$

where

$$Q^2 \frac{dy G_{HT}(y, Q^2)}{dQ^2} = -\frac{9\alpha_s^2}{2R^2} \int_y^{10^{-2}} \frac{dz}{z} [zG(z, Q^2)]^2 \tag{A-3}.$$

## References

- [1] D.J. Gross and F. Wilczek, *Phys. Rev. D* **8** (1973) 3633.
- [2] D.J. Gross and F. Wilczek, *Phys. Rev. D* **9** (1974) 980.
- [3] H. Georgi and H.D. Politzer, *Phys. Rev. D* **9** (1974) 416.
- [4] G. Altarelli and G. Parisi, *Nucl. Phys. B* **126** (1977) 298.
- [5] V.N.Gribov and L.N. Lipatov, *Sov. J. Nucl. Phys.* **15**(1972) 438.
- [6] Yu.L.Dokshitzer, *Sov. Phys. JETP.* **46** (1977) 641.
- [7] G. Parisi and R. Petronzio, *Phys. Lett. B* **62** (1976) 331.
- [8] V.A. Novikov, M.A. Shifman, A.I. Vainshtein, V.I. Zakharov, *JETP Lett.* **24** (1976) 341.
- [9] M. Glück, E. Reya, *Nucl. Phys. B* **130** (1977) 76.
- [10] R. L. Jaffe, *Phys. Rev. D* **11** (1975) 1953.
- [11] A. Le Yaouanc, L. Oliver, O. Pene, and J. C. Raynal, *Phys. Rev. D* **11** (1975) 1272.
- [12] R.J. Hughes, *Phys. Rev. D* **16** (1977) 622.
- [13] J.S. Bell and A.J.G. Hey, *Phys. Lett.B* **74** (1978) 77.
- [14] C.J. Benesh and G.A. Miller, *Phys. Rev. D* **36** (1987) 1344.
- [15] I.C. Cloet, W. Bentz, A.W. Thomas, *Phys. Lett. B***621** (2005) 246.
- [16] M. Glück, E. Reya, A. Vogt, *Z. Phys. C* **48** (1990) 471.
- [17] L.V. Gribov, E.M. Levin and M.G. Ryskin, *Phys. Rep.* **100** (1983) 1.
- [18] A.H. Mueller and J. Qiu, *Nucl. Phys. B* **268** (1986) 427.
- [19] J.C. Collins and J. Kwiecinski, *Nucl. Phys. B* **335** (1990) 89.
- [20] J. Bartels, G.A. Schuler and J. Blumlein, *Z. Phys. C* **50** (1991) 91.
- [21] M. Altmann, M. Glück and E. Reya, *Phys. Lett. B* **285** (1992) 359.
- [22] W. Zhu, *Nucl. Phys. B* **551** (1999) 245 [arXiv:hep-ph/9809391];
- [23] W. Zhu, J.H. Ruan, *Nucl. Phys.B* **559** (1999) 378 [arXiv:hep-ph/9907330v2];

- [24] W. Zhu and Z.Q. Shen, *HEP & NP*, **29** (2005) 109 [arXiv:hep-ph/0406213v3].
- [25] M. Glück, E. Reya, and A. Vogt, *Eur. Phys. J.C* **5** (1998) 461.
- [26] P.D.B. Collins, An Introduction to Regge Theory and High Energy Scattering, *Cambridge University Press* (1977).
- [27] H. Mineo, W. Bentz, N. Ishii, A.W. Thomas, K. Yazaki, *Nucl. Phys. A* **735** (2004) 482.
- [28] V.A. Abramovsky, J.N. Gribov and O.V. Kancheli, *Sov. J. Nucl. Phys.* **18** (1974) 308.
- [29] W. Zhu, D.L. Xue, K.M. Chai and Z.X. Xu, *Phys. Lett. B* **317** (1993) 200.
- [30] J.C. Collins and J.W. Qiu, *Phys. Rev.D* **39** (1989) 1398.
- [31] W. Zhu, *Chin. Phys. Lett.* **16** (1999) 481.
- [32] C.F. von Weizsäcker, *Z. Phys.* **88** (1934) 612.
- [33] E.J. Williams, *Phys. Rev.* **45** (1934) 729.
- [34] V.N Baier, V.S. Fadin and V.A. Khoze, *Nucl. Phys. B* **65** (1973) 381.
- [35] M.S. Chen and P. Zerwas, *Phys. Rev. D* **12** (1975) 187.
- [36] L.N. Lipatov, *Sov. J. Nucl. Phys.* **23** (1976) 338.
- [37] V.S. Fadin, E.A. Kuraev, L.N. Lipatov, *Phys. Lett. B* **60** (1975) 50.
- [38] E.A. Kuraev, L.N. Lipatov, V.S. Fadin, *Sov. Phys. JETP* **44** (1976) 443.
- [39] E.A. Kuraev, L.N. Lipatov, V.S. Fadin, *Sov. Phys. JETP* **45** (1977) 199.
- [40] I.I. Balitsky, L.N. Lipatov, *Sov. J. Nucl. Phys.* **28** (1978) 822.
- [41] I.I. Balitsky, L.N. Lipatov, *JETP Lett.* **30** (1979) 355.
- [42] W. Zhu, *Phys. Lett.* **B389** (1996) 374.
- [43] W.Zhu, J.H. Ruan, J.F. Yang and Z.Q. Shen, *Phys.Rev.D* **68** (2003) 094015.
- [44] J.H. Ruan and W. Zhu, *Phys.Rev.C* **80** (2009) 045209.
- [45] J.H. Ruan and W. Zhu, *Phys. Rev.C* **81** (2010) 055210.
- [46] W. Zhu, J.H. Ruan and F.Y. Hou, *Int. J. Mod. Phys. E* **22** (2013) 1350013.

- [47] H1 Collab. (S. Aid *et al.*), *Nucl. Phys.B* **470** (1996) 3.
- [48] H1 Collab. (C. Adloff *et al.*), *Nucl. Phys. B* **497** (1997) 3.
- [49] H1 Collab. (C. Adloff *et al.*), *Eur. Phys. J.C* **21** (2001) 33 [arXiv:hep-ex/0012053].
- [50] H1 Collab. (C.Adloff *et al.*), *Eur. Phys. J. C* **13** (2000) 609 [arXiv:hep-ex/9908059].
- [51] H1 Collab. (C. Adloff *et al.*), *Eur. Phys. J. C* **19** (2001) 269 [arXiv:hep-ex/0012052].
- [52] ZEUS Collab. (M. Derrick *et al.*), *Z. Phys. C* **69** (1996) 607.
- [53] ZEUS Collab. (M. Derrick *et al.*), *Z. Phys. C* **72** (1996) 399.
- [54] ZEUS Collab. (S. Chekanov *et al.*), *Eur. Phys. J. C* **21** (2001) 443 [arXiv:hep-ex/0105090].
- [55] ZEUS Collab. (J.Breitweg *et al.*), *Phys. Lett. B* **487** (2000) 53 [arXiv:hep-ex/0005018].
- [56] ZEUS Collab. (J. Breitweg *et al.*), *Phys. Lett. B* **407** (1997) 432.
- [57] The New Muon Collab. (M. Arneodo *et al.*), *Nucl. Phys. B* **483** (1997) 3 [arXiv:hep-ph/9610231].
- [58] BCDMS Collab. (A. C. Benvenuti *et al.*), *Phys. Lett. B* **223** (1989) 485 .
- [59] E665 Collab. (M. R. Adams *et al.*), *Phys. Rev. D* **54** (1996) 3006 .
- [60] A. Donnachie and P.V. Landshoff, *Phys. Lett. B* **437** (1998) 408.
- [61] for see A. De Roeck, R.S. Thorne, *Prog. Part. Nucl. Phys.* **66** (2011) 727 [arXiv:1103.0555].
- [62] J.F. Owens, *Phys. Rev. D* **87** (2013) 094012 [arXiv:1212.1702].
- [63] M. Glück, C. Pisano, E. Reya, *Eur. Phys. J.C* **40** (2005) 515;
- [64] P. Jimenez-Delgado, E. Reya, *Phys. Rev. D* **79** (2009) 074023.
- [65] W. Zhu, K.M. Chai and B. He, *Nucl. Phys. B* **427** (1994) 525.
- [66] W. Zhu, K.M. Chai and B. He, *Nucl. Phys.B* **449** (1995) 183.
- [67] E.G.S. Luna, *Braz. J. Phys.* **37** (2007) 84.
- [68] A.A. Natale, *Braz. J. Phys.* **37** (2007) 306.

- [69] Y. M. Cho, *Phys. Rev. Lett.* **46** (1981) 302;
- [70] Y. M. Cho, *Phys. Rev. D* **23** (1981) 2415.
- [71] NA51 Collab. (A. Baldit *et al.*), *Phys. Lett. B* **B332**, 244 (1994);
- [72] FermilabE866/NuSea Collab. (E.A. Hawker *et al.*), *Phys. Rev. Lett.* **80** (1998) 3715.